AD-A237 460

DOCUMENTATION PAGE

Form Approved
OMB No 0704 0188

1a.	1b. RESTRICTIVE MARKINGS
2a.	3. DISTRIBUTION/AVAILABILITY OF REPORT
2b. DECLASSIFICATION/DOWNGRADING SCHEDULE	Approved for public release and sale; its distribution is unlimited.

4. PERFORMING ORGANIZATION REPORT NUMBER(S)	5. MONITORING ORGANIZATION REPORT NUMBER(S)
Technical Report No. 98	

6a. NAME OF PERFORMING ORGANIZATION	6b. OFFICE SYMBOL (If applicable)	7a. NAME OF MONITORING ORGANIZATION
Purdue University Department of Chemistry		Division of Sponsored Programs Purdue Research Foundation

6c. ADDRESS (City, State, and ZIP Code)	7b. ADDRESS (City, State, and ZIP Code)
Purdue University Department of Chemistry West Lafayette, IN 47907	Purdue University West Lafayette, IN 47907

8a. NAME OF FUNDING/SPONSORING ORGANIZATION	8b. OFFICE SYMBOL (If applicable)	9. PROCUREMENT INSTRUMENT IDENTIFICATION NUMBER
Office of Naval Research		Contract No. N00014-91-J-1409

8c. ADDRESS (City, State, and ZIP Code)	10. SOURCE OF FUNDING NUMBERS			
800 N. Quincy Street Arlington, VA 22217	PROGRAM ELEMENT NO.	PROJECT NO	TASK NO	WORK UNIT ACCESSION NO

11. TITLE (Include Security Classification)
Temperature Dependence of Proton Electroreduction Kinetics at Gold(111) and (210) Surfaces

12. PERSONAL AUTHOR(S)
A. Hamelin, L. Stoicoviciu, S.-C. Chang, and M.J. Weaver

13a. TYPE OF REPORT	13b. TIME COVERED	14. DATE OF REPORT (Year, Month, Day)	15. PAGE COUNT
Technical	FROM _____ TO _____	May 31, 1991	

16. SUPPLEMENTARY NOTATION

17. COSATI CODES			18. SUBJECT TERMS (Continue on reverse if necessary and identify by block number)
FIELD	GROUP	SUB-GROUP	proton electroreduction kinetics, temperature dependence-electrocatalytic effect, morphology of cyclic voltammograms

19. ABSTRACT (Continue on reverse if necessary and identify by block number)
Rate-potential data are reported for proton electroreduction on Au(111) and (210) in acidic perchlorate electrolyte over the temperature range 0 -60°C, and examined with regard to the temperature dependence of the transfer coefficient α. Since the Tafel plots exhibit significant curvature (α decreasing with increasing overpotential), the analysis requires information on the temperature-dependent thermodynamics (i.e. the reaction entropy, ΔS°_{rc}) for the proton discharge step. This was estimated from the temperature-dependent voltammetry of reversible proton discharge to form adsorbed hydrogen on platinum. When evaluated at a constant overpotential for the proton discharge step, α for this reaction on both Au(111) and (210) is virtually independent of temperature, both before and after diffuse-layer corrections. An electrocatalytic effect for proton reduction on Au(111) engendered by prior voltammetric oxide formation was also observed. This effect is prevalent at lower temperatures (T ≤ 25°C), and attributed to the formation of surface defects on the basis of recently reported scanning tunneling microscopy (STM) data. These surface structural changes

20. DISTRIBUTION/AVAILABILITY OF ABSTRACT ☐ UNCLASSIFIED/UNLIMITED ☐ SAME AS RPT. ☐ DTIC USERS	21. ABSTRACT SECURITY CLASSIFICATION
22a. NAME OF RESPONSIBLE INDIVIDUAL	22b. TELEPHONE (Include Area Code) | 22c. OFFICE SYMBOL

DD Form 1473, JUN 86   Previous editions are obsolete   SECURITY CLASSIFICATION OF THIS PAGE

19. (cont.)

are also evident in the morphology of cyclic voltammograms obtained in the double-layer region. In harmony with the STM results, these electrochemical effects disappear with time when the potential is held in the double layer region, and more rapidly at higher temperatures.

Temperature Dependence of Proton Electroreduction Kinetics

at Gold(111) and (210) Surfaces

by

A. Hamelin, L. Stoicoviciu, S.-C. Chang, and M. J. Weaver

Prepared for Publication

in the

Journal of Electroanalytical Chemistry

Purdue University

Department of Chemistry

West Lafayette, Indiana 47907

May 1991

Temperature Dependence of Proton Electroreduction Kinetics

at Gold(111) and (210) Surfaces and Annealing of Surface Defects

Antoinette Hamelin, Livia Stoicoviciu

Laboratoire d'Electrochimie Interfaciale du C.N.R.S.

1, Place A. Briand, 92195 Meudon, France

Si-Chung Chang and Michael J. Weaver

Department of Chemistry, Purdue University

West Lafayette, Indiana 47907, U.S.A.

ABSTRACT

Rate-potential data are reported for proton electroreduction on Au(111) and (210) in acidic perchlorate electrolyte over the temperature range 0-60°C, and examined with regard to the temperature dependence of the transfer coefficient α. Since the Tafel plots exhibit significant curvature (α decreasing with increasing overpotential), the analysis requires information on the temperature-dependent thermodynamics (i.e. the reaction entropy, ΔS_{rc}°) for the proton discharge step. This was estimated from the temperature-dependent voltammetry of reversible proton discharge to form adsorbed hydrogen on platinum. When evaluated at a constant overpotential for the proton discharge step, α for this reaction on both Au(111) and (210) is virtually independent of temperature, both before and after diffuse-layer corrections. An electrocatalytic effect for proton reduction on Au(111) engendered by prior voltammetric oxide formation was also observed. This effect is prevalent at lower temperatures (T ≤ 25°C), and attributed to the formation of surface defects on the basis of recently reported scanning tunneling microscopy (STM) data. These surface structural changes are also evident in the morphology of cyclic voltammograms obtained in the double-layer region. In harmony with the STM results, these electrochemical effects disappear with time when the potential is held in the double layer region, and more rapidly at higher temperatures.

We have recently examined in some detail the sensitivity of the kinetics of proton reduction at single-crystal gold electrodes to the surface crystallographic orientation.[1] The rate constants were observed to increase systematically with decreasing potential of zero charge (p.z.c.), or with related properties such as the average surface coordination number. This dependence can be rationalized in terms of variations in the stability of the adsorbed hydrogen reaction intermediate. A significant feature is the excellent stability and reproducibility of the kinetics, especially at the higher-index (more catalytic) surface planes.[1]

Given this reproducibility, which is uncommon among reported electrocatalytic reactions at solid electrodes, it is of interest to examine the manner in which the rate-potential behavior (as embodied in the electrochemical transfer coefficient α) depends upon the temperature. This interest arises in part from recent well-documented examples, especially featuring proton electroreduction, in which α is observed to increase significantly with temperature rather than remain constant as anticipated on some theoretical grounds.[2] We report here electrochemical rate constant-potential data for proton reduction on Au(111) and (210) in 0.09 $\underline{M}$ NaClO$_4$ + 0.01 $\underline{M}$ HClO$_4$ at seven temperatures between 0° and 60°C. Differential capacitance-potential and p.z.c. data are utilized to correct the electrode kinetics for diffuse-layer effects. The results demonstrate how identifying the manner in which α depends upon temperature and its fundamental interpretation can be sensitive to the form of the rate-potential dependence.

The Au(210) face was chosen in view of its excellent reproducibility for proton electroreduction.[1] The proton electroreduction kinetics on the Au(111) face are significantly more sensitive to the surface history, most specifically whether or not formation and removal of an oxide monolayer has

immediately preceded the kinetic measurements.[1]   Apparently related differences in the capacitance-potential behavior are observed on Au(111) under these circumstances that diminish sharply as the temperature is raised.[3] It is therefore of interest to ascertain if corresponding temperature-dependent effects can be discerned upon the proton reduction kinetics. Interest in these phenomena is enhanced by the recent observation by scanning tunneling microscopy (STM) that surface defects are formed transiently on Au(111) by electrochemical oxide formation in acidic media.[4]

EXPERIMENTAL

All experimental work was performed at LEI-CNRS, essentially as described in ref. 1. The reference electrode used for the temperature-dependent kinetic measurements reported here was a reversible hydrogen electrode (RHE) at the same temperature as the working electrode; that is, the temperature of the entire cell was varied by means of a thermostat (isothermal conditions). Nevertheless, potentials reported here for kinetic purposes are versus the saturated calomel electrode (SCE) held at 25°C (i.e. nonisothermal conditions). The latter arrangement is more suitable for data interpretation (vide infra).[5]   The isothermal configuration, however, was utilized experimentally here so to eliminate possible difficulties from thermal liquid junction potentials associated with the presence of protons in the electrolyte (0.09 $\underline{M}$ NaClO$_4$ + 0.01 $\underline{M}$ HClO$_4$); an appropriate correction for the temperature dependence of the reference electrode potential was applied, so to convert to the nonisothermal scale. The capacitance-potential measurements utilized neutral 0.1 $\underline{M}$ NaClO$_4$ electrolyte so to extend the negative range of potentials so to overlap with the proton reduction kinetics; the nonisothermal cell arrangement was therefore used directly in this case.

RESULTS

Upon initial contact with the electrolyte, and after each temperature alteration, the electrode underwent several positive-negative potential cycles at 50 mV s^{-1} from the onset of hydrogen evolution to about 1.35 V vs. SCE. The form of these cyclic voltammograms enable the physical state and cleanliness of the surface to be inspected, and also to confirm that the interfacial temperature had become stable. Some changes in the form of the voltammograms are seen as the temperature is varied for Au(111)[3] and Au(210)[8]. Following the observation of a stable voltammogram on the latter surface at each temperature, the potential was swept in the negative direction at 5 mV s^{-1} so to obtain "steady-state" current density-potential (i-E) data for irreversible proton reduction, as detailed in ref. 1. The observed potential-dependent rate constants, k_{ob} (cm s^{-1}), were extracted by using the relation $k_{ob} = i/FC_b$, where F is Faraday's constant and C_b is the bulk hydrogen ion concentration (0.01 M). Previous measurements have verified that the electrode reaction is indeed first order in protons under the conditions encountered here.[1,10]

The procedure was slightly different for Au(111) in that significantly (up to ca 30%) larger currents for proton reduction at a given overpotential were obtained at lower temperatures ($\leq$ 25°C) if the kinetic measurement was immediately preceded by the voltammetric formation and reduction of an oxide monolayer (i.e. using "long" potential cycles). For this reason, several "short" voltammetric cycles, from -0.3 to 0.8 V vs. SCE at 50 mV s^{-1} were generally undertaken following oxide reduction and prior to the kinetic measurement; such a delay brings about a virtual cessation of this "oxide-induced catalytic" effect. Figure 1 is an example of the observed differences in the kinetics of proton reduction (A) and also the voltammetric response on Au(111) in the double-layer region (B) at a low temperature (1°C) following

such repeated "long" and "short" potential cycling. The solid traces in Figs. 1A and B were obtained immediately following several (3-5) voltammetric cycles which encompass the oxide region (from -0.3 V to 1.35 V vs. SCE), whereas for the dashed curves the prior potential excursions (to 0.8 V vs. SCE) avoided oxide formation and removal.

Besides the significantly larger currents observed for proton reduction for the former ("long cycle") condition (Fig. 1A), noticeable differences are seen in the double-layer voltammetric responses obtained following such long and short cycles (Fig. 1B). In the latter case (dashed curve) a pronounced peak is observed at about 0.3 V vs. SCE in both the positive- and negative-going voltammetric segments, which is less prevalent for the former condition (solid curve). Other differences are seen in the shape of the current-potential curve, which are also reflected in the corresponding differential capacitance-potential data.[3,6,7] (See, for example, Figs. 25 and 38 of ref. 7). Corresponding results to those in Fig. 1, but obtained at an above-ambient temperature (42°C), are shown in Fig. 2. In this case, essentially no differences are seen in the proton reduction kinetics (A) and double-layer voltammetric responses (B) following "short" and "long" potential cycles. At room temperature, such differences are still observed but to a lesser extent. Only kinetic measurements obtained after "short cycles" will be used for the following analysis.

Plots of log k_{ob} versus E for seven temperatures between 0° and 60°C are shown for Au(111) and (210) in Figs. 3 and 4, respectively. The changes in k_{ob} with temperature at a given potential are well outside the experimental uncertainty ($\leq$ ±10%). The lower limit of k_{ob} values evaluated here, ca 5 x 10^{-6} cm s^{-1}, was determined by the onset of measurable faradaic current above the background. The upper limit, ca 1 x 10^{-3} cm s^{-1}, arises from the diminished stability of the measured currents above this point, most likely

associated with hydrogen bubble formation.

Prior to data interpretation, it is advisable to examine the effect of the diffuse double layer upon the kinetics. For this purpose, it is necessary to obtain the potential drop across the diffuse layer, ϕ_2, as a function of E for the different temperatures. This was obtained, as usual, by combining plots of ϕ_2 against the electrode charge density, σ_m, extracted from Gouy-Chapman theory with charge-electrode potential (σ_m-E) data. The latter were obtained by integrating differential capacitance-potential (C_d-E) curves in 0.1 M NaClO$_4$ together with the corresponding pzc values, E_{pzc}, taken from the appropriate C_d-E minima.[1] The E_{pzc} values for Au(111) and Au(210) at 25°C in 0.09 M NaClO$_4$ + 0.01 M HClO$_4$ are approximately 0.24 V and -0.09 V vs. SCE.[1] The variation of the latter with temperature (< 0.5 mV K^{-1}, nonisothermal cell conditions) is almost negligible[8]; this temperature coefficient is slightly larger ($\approx$ 2.5 mV K^{-1}) for Au(111).[3] In the range of σ_m values on Au(210), -12 to -35 μC cm^{-2}, corresponding to the potential range -400 to -750 mV vs. SCE over which the kinetic data were obtained, there is no significant variation of σ_m with temperature within the experimental uncertainties (ca ± 1 μC cm^{-2}). The resulting temperature-dependent ϕ_2-E plots for Au(210) are shown in Fig. 5.

The diffuse-layer corrections were applied to the log k_{ob}-E data in a conventional manner, by plotting log k_{ob} + (F/2.3 RT)Zϕ_2 versus (E-ϕ_2) so to yield double-layer corrected Tafel plots[9]; in this case the reactant charge number, Z, equals +1. Such temperature-dependent corrected Tafel plots for Au(210) are shown in Fig. 6. The slopes of these plots enable the required diffuse layer-corrected transfer coefficients, α_{cor}, to be obtained as a function of potential and temperature from

$$\alpha_{cor} = - \left(\frac{2.3\ RT}{F}\right)\{\partial[\log k_{ob} + (F\phi_2/2.3\ RT)]/\partial(E - \phi_2)\} \qquad (1)$$

These can be compared with corresponding observed or "apparent" transfer coefficients, obtained from

$$\alpha_{ob} = - (\frac{2.3 \ RT}{F}) \ (\partial \ \log \ k_{ob}/\partial E) \tag{2}$$

Although the diffuse-layer corrections exert a substantial influence upon the absolute rate constants (up to ca tenfold), the corresponding effect upon the α values is small, such that commonly $(\alpha_{ob} - \alpha_{cor}) \leq 0.03$. This is especially the case for Au(111), for which the shapes of the observed and corrected Tafel plots are virtually identical within the uncertainties of the rate measurements. Given the greater uncertainties in the p.z.c. values and hence the diffuse-layer corrections for this face, the uncorrected Tafel plots in Fig. 3 are deemed adequate for the present purposes.

DISCUSSION

Before discussing the rate-potential data, it is of interest to consider briefly the observed temperature-dependent effects of oxide formation upon the proton reduction kinetics on Au(111). As noted above, recent in-situ STM measurements for a Au(111) surface in $0.1\underline{M}$ $HClO_4$ at room temperature show that potential cycling so to form and remove at least one oxide monolayer yields significant surface disordering in the form of monoatomic "pits" and terrace edges.[4] Holding the potential subsequently within the double-layer region, however, results in spontaneous removal of these defects within ca 10-15 min. Although corresponding temperature-dependent measurements have not been reported, these findings are entirely consistent with the present results. Thus the occurrence of higher currents for proton reduction on Au(111) would be expected to accompany the formation of surface defects, given that faster kinetics are observed on higher-index faces (and polycrystalline gold),

associated presumably with increased stability of the adsorbed hydrogen intermediate.[1] At lower temperatures $(T \leq 25°C)$, the defects have sufficient temporal stability to affect the electrode kinetic measurements, whereas they are removed too rapidly by spontaneous "annealing" at higher temperatures.

The corresponding temperature-dependent changes in the voltammetric response in the double-layer region are also consistent with this picture. The sharp peaks seen at 0.2 to 0.4 V vs. SCE under "short-cycle" conditions are largely removed by means of "long cycles" at lower temperatures (Fig. 1B). Most likely, these peaks arise from potential-induced surface reconstruction[6,7] which should be altered substantially by extensive formation of surface defects.

At a given temperature, the α_{ob} (and α_{cor}) values for proton reduction diminish significantly with increasing overpotential, especially on Au(210), from values above 0.6 to about 0.4. This α - E dependence could arise from a change in mechanism.[10] It is, however, at least qualitatively also consistent with the expectations of conventional charge-transfer theory in that α should generally decrease with increasing overpotential.[11] (Also see, for example, ref. 12). In order to examine the dependence of α upon temperature in the context of conventional theory it is necessary to evaluate α at a fixed overpotential for the charge-transfer step. This causes no difficulty for reversible single-step reactions since the standard (or formal) electrode potential, $E°$, can be evaluated at each temperature, enabling the overpotential (and hence the free-energy driving force) to be fixed as the temperature is varied.

It is important to recognize that the $E°$, and hence the overpotential in question, refers to the elementary charge-transfer step that determines the measured kinetics. In the present case, at least at higher overpotentials

this is believed to be the proton discharge step[10]

$$H_3O^+ + e^- \rightarrow H_{ad} \qquad (3)$$

where H_{ad} denotes adsorbed hydrogen. While $E°$ for the *overall* hydrogen evolution process is of course measurable, that for reaction (3) unfortunately is unknown. This difficulty can, however, be circumvented by noting that the evaluation of temperature-dependent α values at a fixed (albeit unknown) overpotential only requires a knowledge of the *temperature dependence* of $E°$ rather than its absolute value. Using the present nonisothermal cell arrangement (i.e. with the reference electrode held at a fixed ambient temperature), the temperature dependence of the standard potential can be related to the "reaction entropy" $\Delta S°_{rc}$ (i.e. the entropy change accompanying the redox process) by[13]

$$F(dE°_{ni}/dT) \approx \Delta S°_{rc} \qquad (4)$$

where F is Faraday's constant. If the reaction entropy is (say) zero, then it would be appropriate to examine the α values at a fixed nonisothermal cell potential, E_{ni}, as the temperature is varied. If $\Delta S°_{rc} \neq 0$, the consequent variation in driving force as the temperature is varied can be corrected for by evaluating α at electrode potentials at each temperature such that $(E_{ni} - E°_{ni})$ = constant.

For proton discharge on gold, the $\Delta S°_{rc}$ value for reaction (3) cannot be evaluated since the coverage of adsorbed hydrogen is very low. A rough $\Delta S°_{rc}$ estimate, however, can be extracted for the corresponding process on polycrystalline platinum since well-known peaked voltammograms are obtained that correspond to the formation of distinct states of adsorbed hydrogen (cf. ref. 14). Evaluation of such voltammograms in acidic perchlorate

electrolytes using a nonisothermal cell over the temperature range 0°-60°C yielded (dE°_{ni}/dT) values (obtained from the temperature-dependent shift in the symmetrical hydrogen adsorption peaks) of 0.6 (± 0.1) mV K^{-1} ($\simeq$ 60 J. mol^{-1} K^{-1}). Comparable results, although using a different experimental configuration, are reported in ref. 14.

Armed with this information, we can examine the degree to which α depends upon temperature under conditions of roughly constant overpotential for proton discharge. Table I contains values of α_{ob} and α_{cor} extracted from the experimental rate-potential data on Au(111) and Au(210). These data refer to E_{ni} values of -625 mV and -580 mV vs. SCE, respectively, at 30°C. The E_{ni} values at other temperatures were adjusted away from the value at 30°C by assuming that (dE°_{ni}/dT) - 0.6 mV K^{-1}, thereby correcting for the temperature-dependence driving force. Although somewhat arbitrary, the E_{ni} values were chosen so to correspond to relatively high overpotentials (where proton discharge is most likely the rate-determining step[10]), yet enabling α values to be evaluated reliably over the present temperature range. The differing E_{ni} values chosen at Au(111) and Au(210) reflect the dissimilar rates obtained for these surfaces.

Inspection of Table I shows that the α_{ob} and α_{cor} values extracted on this basis depend only very mildly on the temperature, tending to decrease slightly as T increases. Although different absolute α_{ob} (or α_{cor}) values are observed at other overpotentials given the curvature in the Tafel plots, a similar temperature independence of α is typically obtained by using the above analysis. This finding differs somewhat from most other proton discharge reactions that have been studied, which tend to exhibit significant increases of α with increasing temperature.[2] In some cases, α is found to be approximately proportional to the absolute temperature[2]. This would correspond to α increasing by ca 20% (i.e. by 0.1) over the 60°C temperature

range in Table I, which is clearly not the case here.

Such T-dependent α behavior is often found for charge-transfer reactions involving atom transfer,[2] even though essentially temperature-independent transfer coefficients are usually obtained (as expected from theory) for one-electron outer-sphere electrochemical reactions for which conventional theory should be most applicable.[15,16] It is therefore reasonable to suppose that the interesting temperature dependencies of α obtained for proton and other atom transfer reactions are associated in general with the additional complexities of these processes rather than signaling a more fundamental breakdown of electron-transfer models.

Admittedly, the deduction that α does not vary significantly with temperature for the present systems is somewhat dependent upon the assumed value of (dE°_{ni}/dT). If (dE°_{ni}/dT) is taken as zero, for example, then α_{ob} and α_{cor} are seen to decrease noticeably, by ca 0.06, from 0 to 60°C. Although the (dE°_{ni}/dT) value is an estimate, a probably greater uncertainty is associated with the underlying cause of the marked overpotential dependence of α. As noted above, the validity of the present temperature-dependent analysis, strictly speaking, assumes the occurrence of a single proton-discharge mechanism under the conditions encountered here. Even given such uncertainties, the present analysis does provide evidence that the electrochemical proton discharge process on gold does not necessarily yield significant variations of α with temperature once the likely effects of temperature-dependent driving force are taken into account. Further information on the mechanisms and energetics of this process will be required, however, before more detailed conclusions can be drawn.

References

1. A. Hamelin and M. J. Weaver, J. Electroanal. Chem., 223 (1987), 171.

2. For a recent review, B. E. Conway in "Modern Aspects of Electrochemistry", Vol. 16, B. E. Conway, R. E. White, and J. O'M. Bockris, eds., Plenum Press, New York, 1985, p. 103.

3. A. Hamelin, J. Electroanal. Chem., 210 (1986), 303.

4. D. J. Trevor, C. E. D. Chidsey, D. N. Loiacono, Phys. Rev. Lett., 62 (1989), 929.

5. M. J. Weaver, J. Phys. Chem., 83 (1979), 1748.

6. A. Hamelin, J. Electroanal. Chem., 142 (1982), 299.

7. A. Hamelin in "Modern Aspects of Electrochemistry", Vol. 16, B. E. Conway, R. E. White, and J. O'M. Bockris, eds., Plenum Press, New York, 1985, p. 1.

8. A. Hamelin, L. Stoicoviciu, and F. Silva, J. Electroanal. Chem., 229 (1987), 107.

9. P. Delahay, "Double Layer and Electrode Kinetics", Interscience, New York, 1965, Chapter 9.

10. G. J. Brug, M. Sluyters-Rehbach, J. H. Sluyters, A. Hamelin, J. Electroanal. Chem. 181 (1984), 245.

11. R. A. Marcus, J. Chem. Phys., 43 (1965), 679.

12. J. T. Hupp; M. J. Weaver, J. Phys. Chem., 88 (1984), 6128.

13. E. L. Yee, R. J. Cave, K. L. Guyer, P. D. Tyma, M. J. Weaver, J. Am. Chem. Soc., 101 (1979), 1131.

14. B. E. Conway, H. Angerstein-Kozlowska, W. B. A. Sharp, J. Chem. Soc. Far. Trans. I, 74 (1978), 1373.

15. M. J. Weaver, J. Phys. Chem., 83 (1979), 1748.

16. Z. Nagy, N. C. Hung, R. M. Yonco, J. Electrochem. Soc., 136 (1989), 895.

TABLE I   Representative Transfer Coefficients for Proton Reduction over the Temperature Range 0-60°C on Au(111) and Au(210) in 0.9 $\underline{M}$ NaClO$_4$ + 0.01 $\underline{M}$ HClO$_4$

Temperature	Au(111)[a]		Au(210)[b]	
	α_{ob}	α_{cor}	α_{ob}	α_{cor}
0	0.55	0.53	0.62	0.60
11	0.54	0.53	0.62	0.60
20			0.61	0.58
22	0.54	0.52		
30	0.54	0.52	0.59	0.56
40	0.54	0.51	0.60	0.57
50	0.53	0.50		
53			0.60	0.57
60	0.53	0.50		

[a]Evaluated at nonisothermal cell potentials equal to [-625 mV vs. SCE + 0.6 (T-30°C)mV], where T is temperature (°C).

[b]Evaluated at nonisothermal cell potentials equal to [-580 mV vs. SCE + 0.6(T -30°C)mV], where T is temperature (°C).

FIGURE CAPTIONS

Fig. 1

A. Current-potential curves (at 5 mV s^{-1}) at low overpotentials for proton reduction on Au(111) in 0.1 $\underline{M}$ HCLO$_4$ at 1°C. Solid curve obtained after 6 "long cycles" at 50 mV s^{-1} between -0.3 V and 1.4 V vs. SCE. Dashed curves obtained after 6 "short cycles" i.e. only to 0.8 V vs. SCE. Currents obtained during negative- and positive-going potential scans are virtually identical.

B. Cyclic voltammograms obtained in "double-layer region" (note expanded current scale) following "long " and "short cycles" (solid and dashed curves), performed as in A.

Fig. 2

As in Fig. 1, but at 42°C.

Fig. 3

Plots of logarithm of the observed rate constant, k_{ob}, versus electrode potential for proton reduction on Au(111) at various temperatures. Electrolyte is 0.09 $\underline{M}$ NaCLO$_4$ + 0.01 $\underline{M}$ HCLO$_4$. Reference electrode is SCE at room temperature. Key to temperatures: ●, 0.5°C; O, 11°C; ■,22°C; □, 31°C; ▲, 41°C; △,50°C; ▼,60°C.

Fig. 4

As for Fig. 3, but for Au(210). Key to temperatures: ●, 0°C; O, 11°C; ■, 20°C; □, 30°C; ▲, 41°C; △, 53°C; ▼, 60°C.

Fig. 5

Plots of potential across diffuse layer versus electrode potential for Au(210) in 0.09 $\underline{M}$ NaCLO$_4$ + 0.01 $\underline{M}$ HCLO$_4$ at various temperatures. Obtained from differential capacitance - electrode potential data along with potentials of zero charge and Gouy-Chapman theory (see text). Key to temperatures as in Fig. 4.

Fig. 6

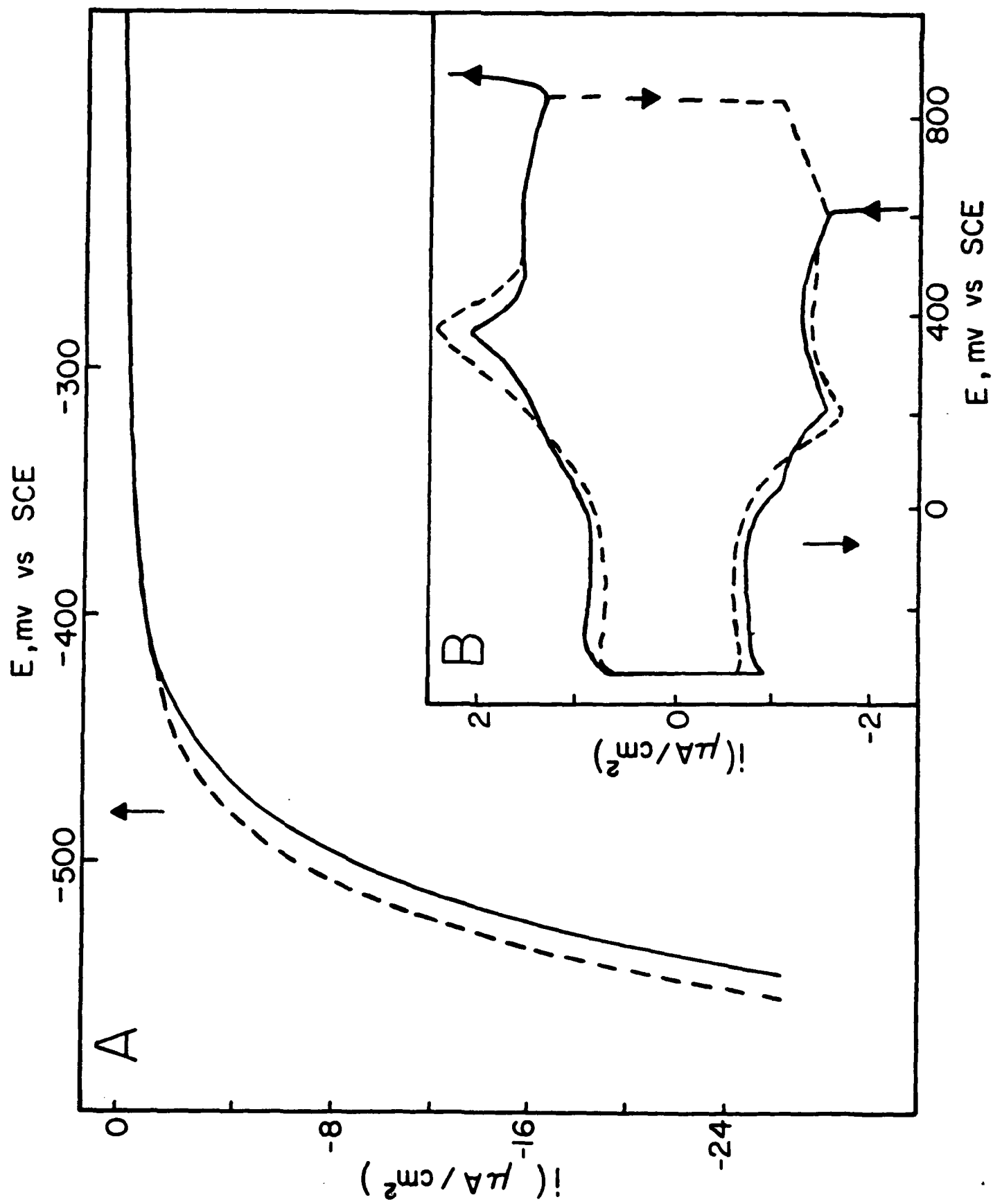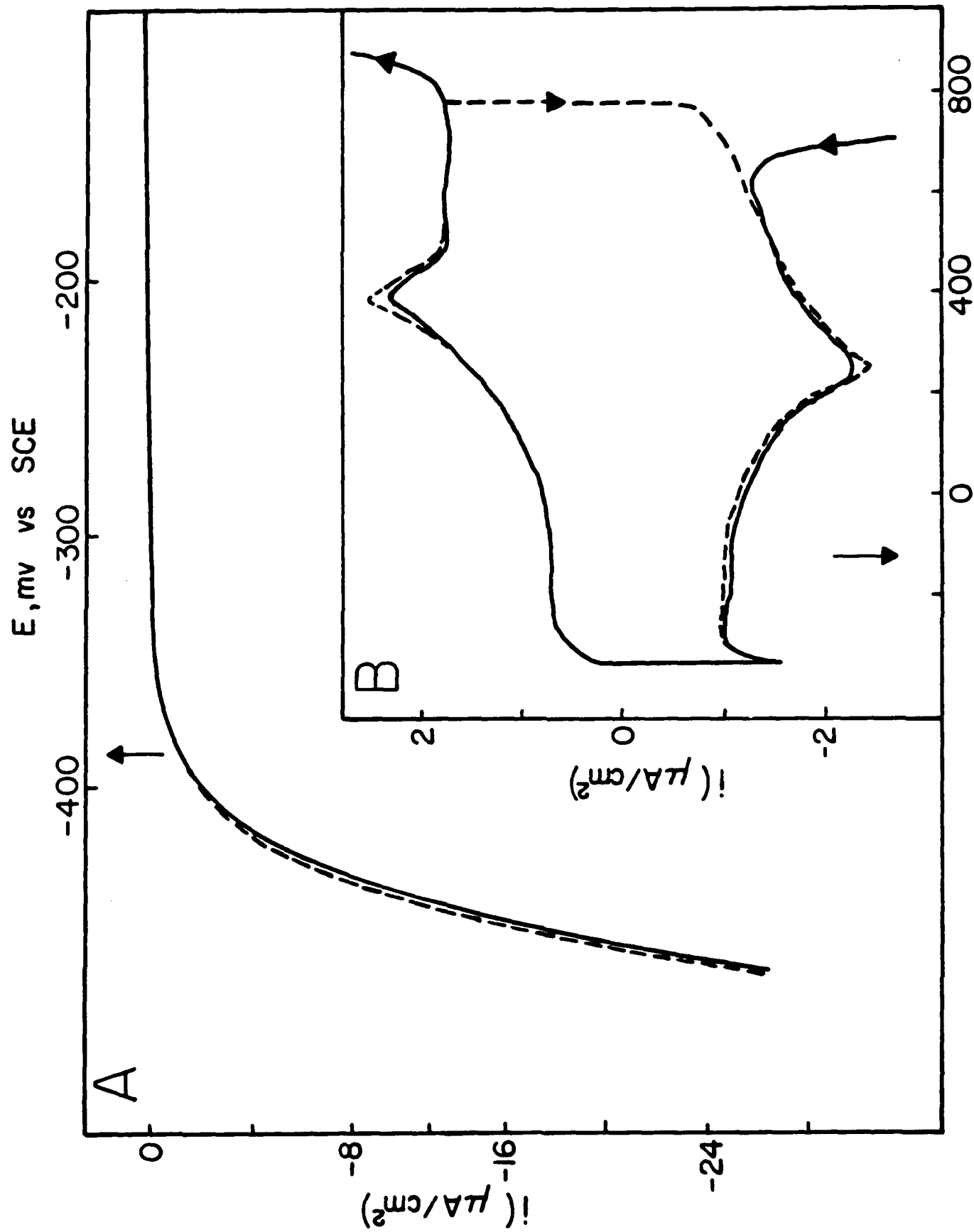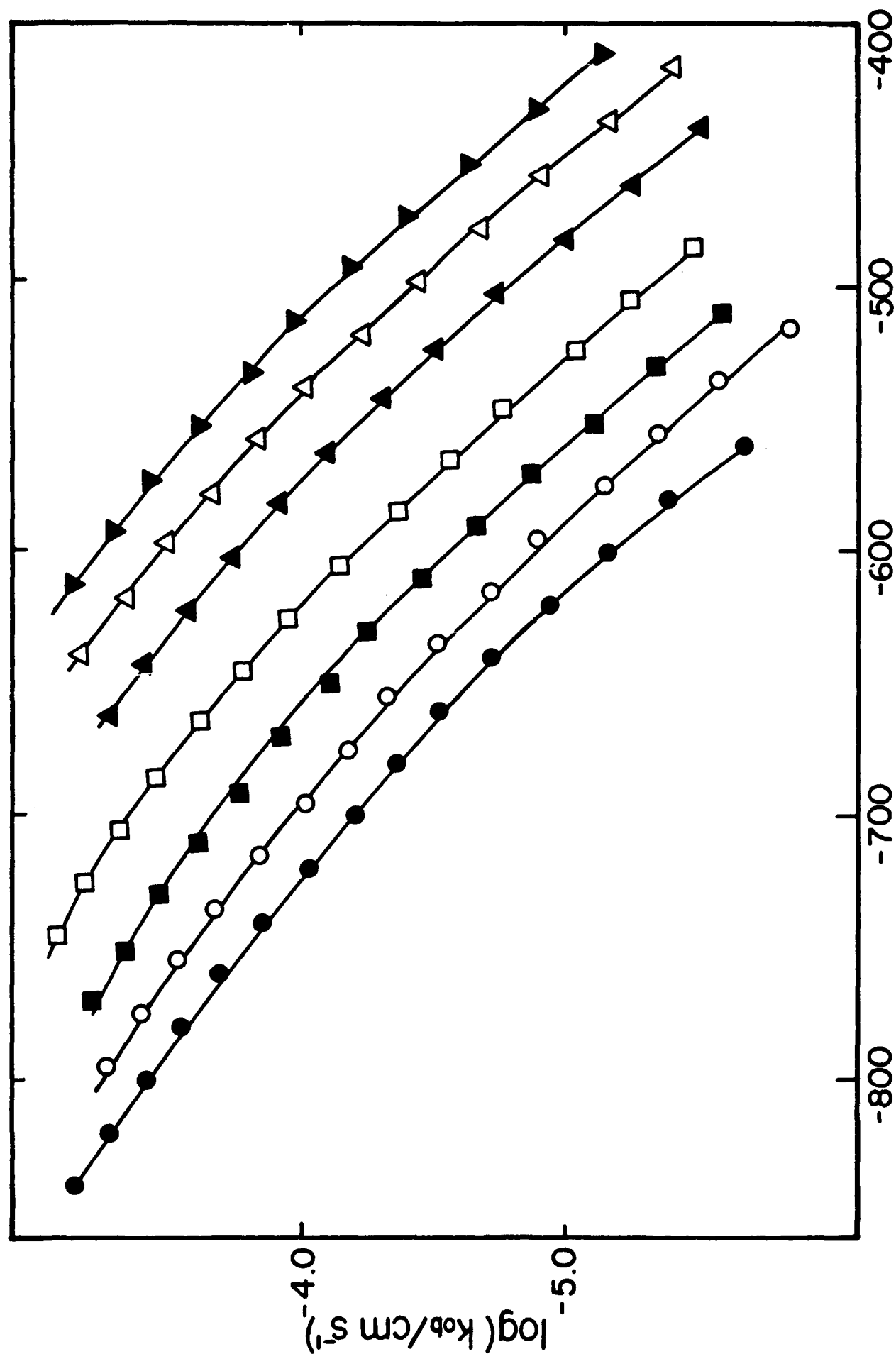As in Fig. 4, but after double-layer corrections using ϕ_2 - E data shown in Fig. 5.

Fig. 1

Fig. 2

Fig. 3

Fig. 4

Fig. 5

Fig. 6